

Partitioning of Liquid-ordered / Liquid-disordered Membrane Microdomains Induced by the Fluidifying Effect of 2-Hydroxylated Fatty Acid Derivatives.

**Maitane Ibareguren<sup>a,1</sup>, David J. López<sup>a,1</sup>, José A. Encinar<sup>b</sup>, José M. González-Ros<sup>b</sup>, Xavier Busquets<sup>a</sup> and Pablo V. Escribá<sup>a</sup>**

<sup>a</sup>Laboratory of Molecular Cell Biomedicine, University of the Balearic Islands-Lipopharma Therapeutics, S.L., Palma, Spain.

<sup>b</sup>Molecular and Cell Biology Institute, Miguel Hernández University, Elche, Spain.

To whom correspondence should be addressed:

Pablo V. Escribá, PhD., Laboratory of Molecular Cell Biomedicine, Department of Biology, University of the Balearic Islands, Crta. Valldemossa km. 7.5, 07122, Palma (Spain). Tel.: +34-971 17 33 31; Fax +34-971 17 31 84; E-mail: pablo.escriba@uib.es

David J. López, PhD., Laboratory of Molecular Cell Biomedicine, Department of Biology, University of the Balearic Islands, Crta. Valldemossa km. 7.5, 07122, Palma (Spain). Tel.: +34-971 17 33 31; Fax +34-971 17 31 84; E-mail: davidlopez\_95@hotmail.com

## **Abstract**

Cellular functions are usually associated with the activity of proteins and nucleic acids. Recent studies have shown that lipids modulate the localization and activity of key membrane-associated signal transduction proteins, thus regulating the cell's physiology. Membrane Lipid Therapy aims to reverse cell dysfunctions (i.e., diseases) by modulating the activity of membrane signaling proteins through regulation of the lipid bilayer structure. The present work shows the ability of a series of 2-hydroxyfatty acid (2OHFA) derivatives, varying in the acyl chain length and degree of unsaturation, to regulate the membrane lipid structure. These molecules have shown greater therapeutic potential than their natural non-hydroxylated counterparts. We demonstrated that both 2OHFA and natural FAs induced reorganization of lipid domains in model membranes of POPC:SM:PE:Cho, modulating the liquid-ordered/liquid-disordered structures ratio and the microdomain lipid composition. Fluorescence spectroscopy, confocal microscopy, Fourier transform infrared spectroscopy and differential detergent solubilization experiments showed a destabilization of the membranes upon addition of the 2OHFAs and FAs which correlated with the observed disordering effect. The changes produced by these synthetic fatty acids on the lipid structure may constitute part of their mechanism of action, leading to changes in the localization / activity of membrane proteins involved in signaling cascades, and therefore modulating cell responses.

**Keywords:** Fatty acid; Lipid raft; Membrane lipids; Membrane structure; Membrane fluidity; Membrane Lipid Therapy.

## 1. Introduction

The length and degree of unsaturation of natural fatty acids has been associated with their impact on membrane lipid structure [1] and human health [2]. In recent years, dietary recommendations have been made to decrease saturated and trans-fatty acids due to their negative cardiovascular effects, while mono- and polyunsaturated fatty acids are recommended for their cardio-protective benefits [3]. During the last few years, a number of <sup>2</sup>OHFAs have been rationally designed for the treatment of cancer, inflammation, Alzheimer's disease, obesity, diabetes, spinal cord injury, etc. Some data available indicate that the mechanism of action of these 2OHFAs is related to their capacity to modulate the membrane lipid structure [4-6] but the molecular bases of the differential effects of these fatty acids remain largely unknown. The *in vitro* and *in vivo* studies with these 2OHFAs show that they have greater therapeutic effects than the natural, non-hydroxylated counterparts [7-9]. In this context, 2-hydroxylinoleic and 2-hydroxyoleic acid are currently being developed for the treatment of cancer (preclinical and phase I/II clinical trials, respectively). Moreover, 2-hydroxyoleic acid, a synthetic monounsaturated fatty acid, is under preclinical development for the treatment of spinal cord injury, hypertension, diabetes and obesity. 2-Hydroxyarachidonic acid has been observed to possess anti-inflammatory effects and 2-hydroxydocosahexaenoic acid has aroused as an interesting candidate to revert the cognitive deficiencies associated to neurodegenerative processes such as Alzheimer's disease [6, 10].

2-Hydroxyoleic acid, which is currently being investigated in humans for the treatment of glioma, has a potent antitumoral effect both *in vitro* [11] and *in vivo* [12]. Its pharmacological anticancer activity has been associated with a dual-mode action. On the one hand, this molecule induces important changes on the lamellar-to-nonlamellar phase transition that provoke membrane translocation and activation of PKC $\alpha$  [13]. On the other hand, 2-hydroxyoleic acid induces important changes in membrane-lipid composition that cause Ras translocation from the plasma membrane to the cytoplasm followed by autophagic cell death; however, its molecular mechanism of action is not fully understood [12, 14].

Here, we have studied by means of different biophysical techniques the effect of various 2OHFAs on the membrane lipid structure. It is known that alterations in the plasma membrane structure by lipid molecules can modify cell signaling events [15]. Indeed, several compounds act by regulating signal transduction through a new therapeutic approach named Membrane Lipid Therapy, which aims to the regulation of the membrane lipid organization through structure-function principles [7, 16, 17]. Changes in the membrane physico-chemical properties, such as the lateral pressure [18], membrane fluidity [19] or phase behavior [16], regulate the localization and activity of relevant signaling proteins, which results in the regulation of gene expression and reversion of the pathological state within the cell [7].

Anesthetics, such as ketamine, are classical examples of drugs that alter the cell signaling processes by modulating the lipid membrane structure [20]. Those structural changes in the lipid bilayer may alter the function of membrane peripheral and integral proteins such as ion channels, hence blocking neurotransmission and leading to anesthesia and analgesia [21]. Oleamide, an amide derivative of the oleic fatty acid, has shown to perturb the fluidity of lipid membranes, thus leading to the regulation of receptors that activate G proteins and thereby playing a role in alertness and sleep [22]. Besides, membrane lipid structure has also been described to affect enzyme activity rates, e.g., sphingomyelinases, which hydrolyze SM to give rise to the apoptosis-related sphingolipid ceramide [23]. It has been observed that their maximum activity rates increase (i) at high temperatures (> 42 °C), that is, when transition temperature of SM from gel-to-fluid ( $T_m$ ) has occurred or (ii) when  $T_m$  is decreased by the presence of other lipids such as PC or PE [24].

Lipid rafts are SM and Cho-rich  $L_o$  membrane microdomains that play an important role in cell signaling [25]. Since the discovery of these lipid structures, extensive research provided evidence that they are implicated in the pathogenesis of a variety of conditions [26] such as neurological diseases including Alzheimer's [27], Parkinson's [28] and prion diseases [29], cardiovascular diseases, immune disorders such as systemic lupus erythematosus [30] and HIV infection [31]. Lipid rafts have been also implicated in signaling pathways in cancer progression [32], but how these  $L_o$  microdomains affect the adhesion and migration of invasive cancer cells remains to be determined hitherto [33]. The present study shows the ability of different 2OHFAs to induce important changes in the lipid structure and in the composition and proportion of  $L_o/L_d$  (i.e., raft-like-to-non-raft ratio) microdomains. These regulatory effects can cause relevant modifications in the localization of signaling proteins and may be part of the mechanism of action involved in the therapeutic effects exerted by 2OHFAs.

## **2. Material and methods**

### *2.1. Materials*

POPC, liver bovine PE, egg chicken SM, Cho, and NBD-PE were from Avanti Polar Lipids (Alabaster, AL). Triton X-100, DMSO, OA, SA, LA,  $\alpha$ LNA,  $\gamma$ LNA and ARA were purchased from Sigma-Aldrich (St. Louis, MO). DiI was from Invitrogen (Eugene, OR). Bovine GM1 and 2OHSA were from Larodan (Malmö, Sweden). EPA and DHA were obtained from BASF Pharma (Callanish, UK). 2OHOA, 2OHLA, 2OH $\alpha$ LNA, 2OH $\gamma$ LNA, 2OHARA, 2OHEPA and 2OHDHA were kindly provided by Lipopharma Therapeutics S.L. (Palma, Spain). Chloroform, methanol, n-hexane, acetic acid and diethylether were bought to Scharlab (Barcelona, Spain). Silica G60 20x20 cm plates were from Merck (Darmstadt, Germany) and 200 nm Anotop filters were purchased from Whatman (Kent, United Kingdom).

## 2.2. Preparation of lipid vesicles

POPC:PE:SM:Cho (1:1:1:1; mol ratio) LUVs were prepared in a buffer solution containing 10 mM Hepes, 1 mM EDTA, 100 mM NaCl, pH 7.4 using an extruder device equipped with 200 nm filters as previously described [34]. Quantitative analysis of the lipid composition of LUV was performed as described elsewhere [35] and data showed that the final composition did not significantly differ from the initial lipid mixture (see Fig. 8F).

## 2.3. Lipid phase separation studies

Fatty acid-induced phase separation was monitored by the NBD-PE self-quenching method [36]. Briefly, vesicles containing 5 mol% NBD-PE show an attenuated fluorescence signal due to fluorescence self-quenching when the local concentration of the fluorophore increases, i.e., when this synthetic lipid is segregated out the  $L_o$  to  $L_d$  domains. Monitoring of NBD fluorescence was carried out with a Varian Cary Eclipse Fluorescence Spectrophotometer (Palo Alto, CA). 2 ml of 0.1 mM LUVs were excited at 475 nm and the fluorescence was monitored at 530 nm in quartz cuvettes at room temperature under continuous stirring. The slit widths were 2 nm for both excitation and emission and the fluorescence signal was normalized to the initial fluorescence value of each kinetic experiment. Fatty acids diluted in DMSO were added to the liposome mixture at concentrations ranging from 15 to 45 mol%, which are well below the doses of experiments using cell lines [12, 14]. In addition, according to previous observations, 20HOA treatment of glioma and lung cancer cells causes the synthetic molecule to account for ~15% of the fatty acids within the cells [37].

## 2.4. GUVs preparation and fluorescence microscopy

GUVs were prepared using the electroformation method [38]. For this purpose, lipid solutions containing 0.3 mM total lipid supplemented with 0.4 mol% DiI or 5 mol% NBD-PE were prepared in chloroform:methanol (2:1, v/v). DiI probe is localized preferentially to  $L_d$  phases [39], as well as NBD-acyl chain labeled PE. Three microliters of the lipid mixture were added on the surface of platinum electrodes and solvent traces were removed under high vacuum for 60 minutes. The electrodes were covered with 400  $\mu$ l of 25 mM Hepes buffer, pH 7.4, previously heated at 50 °C. The platinum wires were connected to an electric wave generator at 50 °C under the following AC field conditions: 500 Hz, 0.22 V for 5 min; 500 Hz, 1.9 V for 20 min and finally 500 Hz, 5.3 V for 90 min. After GUVs formation, the cuvette containing the electrodes was placed on a Leica TCS SPE inverted confocal fluorescence microscope (Barcelona, Spain). The excitation wavelengths used were 488 nm and 532 nm for NBD-PE and DiI, respectively. When required, fatty acids dissolved in DMSO were added to a final concentration of 0.135 mM and changes in the morphology and fluorescence of vesicles attached to the platinum wire were monitored.

## 2.5. FTIR spectroscopy

Fifty microliters of lipid samples in 5 mM Hepes buffer, pH 7.4 containing 0.5 mM EDTA, 50 mM NaCl were dehydrated in a speed vac Savant rotary evaporator and suspended in 25  $\mu$ l of D<sub>2</sub>O to avoid the interference of H<sub>2</sub>O infrared absorbance (1645 cm<sup>-1</sup>). Samples were hydrated overnight at a temperature of 32 °C before starting the acquisition of the FTIR spectra. Sample measurements were performed in a liquid demountable cell (Harrick, Ossining, NY, USA) equipped with CaF<sub>2</sub> windows and 25-mm-thick Mylar spacers. FTIR spectra were acquired on a spectrometer IF66/s (Bruker Optics Inc.), equipped with deuterated triglycine sulfate (DTGS) detectors. The sample chamber was constantly purged with dry air. A minimum of 100 scans per spectra were taken, averaged, apodized with a Happ-Genzel function and Fourier-transformed to give a nominal resolution of 2 cm<sup>-1</sup>. Self-deconvolution was performed using a Lorentzian bandwidth of 18 cm<sup>-1</sup> and a resolution enhancement factor of 2.0. Samples were scanned in the temperature range of 20-70 °C, every 2 °C. The duration of a complete heating cycle was of approximately 3 h. Afterwards, samples were cooled and equilibrated at 20 °C to check the reversibility of the transitions. Buffer contributions were subtracted from the individual spectra, and the resulting spectra were used for analysis [40].

## 2.6. Sigmoidal data fitting analysis

Certain infrared and dichroism data presenting a sigmoid behavior cannot be satisfactorily explained with the typical Boltzmann equation, especially if they have big negative or positive sloping bottom and top plateau. From the Boltzmann equation we have developed a new equation that takes into account the positive or negative plateau.

$$\text{Boltzmann} \Rightarrow y = A2 + (A1-A2)/(1 + \exp((x-x0)/dx))$$

$$\text{Boltzmann Modified} \Rightarrow y = A2+B2*x + (A1+B1*x-A2-B2*x)/(1+\exp((x-x0)/dx))$$

Where A1 is the initial value (left horizontal asymptote), B1 is the slope for the initial asymptote, A2 is the final value (right horizontal asymptote), B2 is the slope for the final asymptote, x0 is the center (point of inflection), and dx is the width (the change in X corresponding to the most significant change in Y values). Curve fitting analysis using "Boltzmann Modified" equation was performed with OriginLab 7.0.

## 2.7. Determination of lipid composition in Lo and Ld membrane domains

One milliliter of LUVs (containing 2.5 mM of lipid) composed of POPC:PE:SM:Cho (1:1:1:1; mol ratio) + 1 mol% GM1 were incubated in the absence or presence of 15 mol% of various FAs and 2OHFAs at room temperature for 30 min under continuous stirring. Concentrations below 2 mol% GM1 do not modify the lipid membrane structure [41], so it was added to the lipid mixture as a marker

for DRM fractions [42]. Vesicles were incubated at 4 °C for 1 h in the presence of 1 % Triton X-100 (w/v) and the DRM fraction was separated from detergent-lipid mixed micelles by ultracentrifugation (80,000 g, 5 h) at 4 °C. The pellet (DRM) was suspended in 500 µl of water, both pellet and supernatant were lyophilized overnight and lipids were separated on thin-layer chromatography plates [43]. Briefly, two consecutive developments with chloroform:methanol:water (60:30:5; v:v:v) were done: the solvent front was left to reach the upper part of the plate for the first run following a second development until the solvent covered half of the plate. A third separation was performed in n-hexane:diethylether:acetic acid (80:20:1.5; v:v:v). Plates were charred with a 5% CuSO<sub>4</sub>/ 4% H<sub>3</sub>PO<sub>4</sub> solution and spots were developed at 180 °C for 15 min. Lipid quantification was accomplished by image analysis in a GS-800 densitometer using the Quantity One software from Bio-Rad Laboratories (Hercules, CA).

### 3. Results

#### 3.1. Unsaturated 2OHFAs induce Lo/Ld microdomain reorganization

Time course fluorescence kinetics were recorded in LUVs composed of POPC:PE:SM:Cho (1:1:1:1; mol ratio) containing 5 mol% NBD-PE upon addition of 15, 30 and 45 mol% of 2OHOA (Fig. 1A). At room temperature, these quaternary lipid mixture membranes display lateral lipid heterogeneity, i.e., distinct lipid domains are formed [44]: one Lo, lipid raft-like, phase enriched in SM and Cho, and another domain enriched in the Ld-forming lipids PE and POPC. The acyl chain-labeled NBD-PE has a preference for the more fluid and disordered phases as shown in Fig. S1 and colocalizes with the also Ld-preferring DiI probe [39]. The addition of 2OHOA to the lipid vesicles induced significant increases of the fluorescence intensity in a concentration-dependent manner, while the DMSO did not have any effect on NBD-PE fluorescence (Fig. 1A). Addition of 15 mol% of any of the hydroxylated fatty acid derivatives, with the exception of the saturated fatty acid 2OHSAs, induced a high increase in fluorescence signal (Fig. 1B); subsequent additions of the unsaturated, 2OHFAs, although to a lesser extent, produced further increases of the fluorescence signal (data not shown). All non-hydroxylated fatty acid derivatives but SA, also induced an increase in the fluorescence intensity (Fig. 1C) caused by the disordering effect within the membrane upon insertion of the FA molecules. NBD-PE fluorescence was reduced caused by self-quenching due to a heterogeneous distribution of the fluorophore accumulation in Ld domains; however, after insertion of 2OHFA and FA in the lipid bilayer the fluorescence was increased due to the more homogeneous lipid reorganization.

The highest disordering effect was caused by OA and 2OHOA among the natural and 2-hydroxylated fatty acid derivatives, respectively. Thus, the presence of an 18-carbon acyl chain in combination with a single *cis* double bond possessed the most potent reorganizing effect on the used

model membranes. Further increase in the number of carbon atoms or in the number of double bonds induced significant homogeneous redistribution of lipid components in the membrane although to a lesser extent compared with OA and 2OHOA.

### *3.2. 2OHFAs induced structural changes of model membranes observed by confocal fluorescence microscopy*

The time sequence of the effects of 2OHFA derivatives on POPC:PE:SM:Cho (1:1:1:1; mol ratio) vesicles is shown in Figure 2. DiI partitions preferentially into the more disordered Ld domains enriched in PE and POPC, thus at time 0 min, yellow (Ld) and dark (Lo, lipid raft-like) domains coexist under the experimental conditions used, which agrees with previous studies [39]. However, after addition of the 2OHFAs, the proportion of Ld domain increased with time, until apparent disappearance of Lo domains. Figure 3 shows the relative lengths of the Ld and Lo domains at the confocal equatorial plane as a relative measurement of the Ld and Lo size through the incubation time. Before the addition of 2OHSA, 2OHOA, 2OHARA and 2OHDHA, vesicles showed a heterogeneous distribution of lipids in which ~50% of the perimeter was occupied by Lo and the other half by Ld structures. Upon addition of the 2OHFA derivatives, quantification of Lo and Ld domains showed a continuous reduction of Lo structures that correlated with the increase of Ld (DiI-containing) domains. Interestingly, digital analysis of the overall fluorescence in vesicles showed a slight tendency to increase, although without significant differences, after incubation of the 2OHFAs (Table 1). Figure S1 shows the partition of DiI and acyl chain-labeled NBD-PE in GUVs composed of POPC:PE:SM:Cho (1:1:1:1; mol ratio). Both fluorescent probes localized in the more disordered domains, demonstrating a similar phase partition behavior and a correlation between the results observed by fluorescence spectroscopy (Fig. 1) and confocal microscopy (Fig. 2 and 3). The NBD-PE molecule with the fluorescence probe linked to the hydrophilic headgroup has been elegantly designed as a marker for lipid-rafts [45]; however, it has also been proven that the NBD fluorophore attached to the acyl chain of PE, as the one used in the present work, imposes steric and polarity constraints in the hydrophobic region of lipid bilayer [46]. The result is the almost perfect exclusion of acyl chain-labeled phospholipids from ordered lipid phases and their preferential accumulation into the disordered domains.

Concerning the changes induced in the vesicles structure, the external addition of 2OHFAs in a GUV suspension caused the following effects: (i) in vesicles with coexisting Lo and Ld domains, the Lo phase area decreased or eventually faded away, giving rise to an apparently homogeneous single Ld structure; (ii) vesicles in contact with 2OHOA lost the spherical shape and became oval. Regarding the naturally occurring, non-hydroxylated FAs, the effect is similar to that of the hydroxylated



counterparts (Fig. 4), that is, amount of the DiI-stained (Ld) region increased at the same time that the proportion of dark, lipid raft-like (Lo) domain decreased and apparently disappeared.

### *3.3. Effects of FA and 2OHFA derivatives on membrane lipid structure by Fourier Transform Infrared Spectroscopy*

The effect of unsaturated FAs and their 2-hydroxy derivatives on the lipid membrane was studied by monitoring the temperature-dependent responses in several characteristic bands in the infrared spectra of the samples. The phospholipid carbonyl stretching band, probing the interfacial region of the lipid membrane, shows two component bands at 1745 and 1722  $\text{cm}^{-1}$ , respectively, upon self-deconvolution of the original spectra. These two bands are assigned to dehydrated (1745  $\text{cm}^{-1}$ ) and hydrated (1722  $\text{cm}^{-1}$ ) carbonyl groups [47]. As shown in Figure 5 (panels A - C) and Figure 7A, the intensity of the hydrogen-bonded component (lower frequency) in the POPC:PE:SM:Cho quaternary mixture was greater than that from the dehydrated one. The 1745  $\text{cm}^{-1}$ /1722  $\text{cm}^{-1}$  ratio decreased as the temperature increased up to 55 °C, where it acquired a sigmoid-like behavior with an initial increase and a subsequent decrease in the signal ratio, characteristic of a new phase transition. The best fit of the data to a modified Boltzmann equation (see Experimental Procedures) allowed us to calculate a phase transition temperature of 62.3 °C. Individual components in our quaternary matrix, such as egg-SM and liver-PE, experience transitions from lamellar-to-nonlamellar phases. For instance, egg yolk-PE alone presents a transition from the liquid-crystalline ( $L_{\alpha}$ ) to the inverted hexagonal ( $H_{II}$ ) phase at 28 °C [48]. Bovine brain SM can give raise to a nonlamellar phase transition at high temperature and the inclusion of 20 mol% egg-PC strongly increases it up to 63 °C [49]. More recent studies have shown two transition for 18:1-SM:Cho mixtures at 35-37 °C and 95 °C, but none were related to non-lamellar phases, as  $^{31}\text{P}$ -NMR spectra for these range of temperatures are typical of lamellar phases [50]. Thus, we cannot assigned the transition observed at 62.3 °C in the carbonyl signal ratio from our quaternary mixture to a lamellar to nonlamellar phase transition of the SM component, though undoubtedly SM is involved in the transition. Such involvement was unambiguously confirmed by monitoring of the amide I band region of the spectra (Fig. 6), in which the only contribution from the components of our quaternary mixtures arises from the amide bond in SM [51] and shows an abrupt increase in band frequency with a midpoint temperature of 68 °C.

The addition to the lipid vesicles of either FA or 2OHFA derivatives had similar effects on the phospholipid carbonyl band, regardless the hydrocarbon chain length or the number of double bonds. In all cases, hydration of the carbonyl groups increased, both before and after the phase transition and the transition temperatures decreased (see Fig 5 A-C). A similar conclusion on the effects of FA and 2OHFA derivatives in decreasing the transition temperatures was derived from the monitoring of the SM-specific, amide I spectral band (Figure 6 and 7C).

The region 3000-2800  $\text{cm}^{-1}$  of the infrared spectra (Figure 7B) includes several bands resulting from lipids acyl chains, mainly terminal methyl groups (asymmetric stretch at 2956  $\text{cm}^{-1}$  and symmetric stretch at 2875  $\text{cm}^{-1}$ ) and all the methylene groups (antisymmetric stretch at 2920  $\text{cm}^{-1}$  and symmetric stretch at 2850  $\text{cm}^{-1}$ ). The absolute frequency of this band is sensitive to the conformational order of the acyl chain and to the trans-gauche isomerization of the lipids [52]. In addition, the increase in width of these bands is characteristic of phospholipid hydrocarbon chain-melting phase transitions and arises from the increase in hydrocarbon chain mobility and conformational disorder that occur when all-trans polymethylene chains melt [52]. The analysis of the symmetric methylene band (2850  $\text{cm}^{-1}$ ) for our samples reveals a similar behavior to that evidenced from the carbonyl and the amide I bands. Any of the three non-hydroxylated or the corresponding hydroxylated fatty acids reduced the phase transition temperature and increased the methylene frequency between 0.5 and 1.5  $\text{cm}^{-1}$ , depending on each fatty acid (see Fig. 5 D - F). A change in frequency was also accompanied by an increase in the width of the  $\text{CH}_2$  symmetric stretching band in the presence of both FA and 2OHFA (data not shown).

#### 3.4. Effects of FAs and 2OHFAs on the Lo/Ld domain ratio

Model membranes (LUVs) with or without 15 mol% of 2OHFAs or FAs were treated with the anionic detergent Triton X-100 at 4 °C with constant stirring, following centrifugation to separate the DRM (pellet) from the solubilized fraction (supernatant). Vesicles made from the quaternary lipid mixture and treated with vehicle (DMSO) and 1% Triton X-100 (w/v) were used as control. The proportion of lipid raft-like, Lo structures (DRM fraction), decreased in the presence of 2-hydroxylated (Fig. 8A) and non-hydroxylated (Fig. 8B) fatty acids compared to the control vesicles. Both FAs and 2OHFAs significantly reduced the amount of Lo domains from *ca.* 50% to *ca.* 38-42% of the total lipid amount in the vesicles. The *ca.* 10% reduction in the DRM fraction might not reflect the dramatic decrease (*ca.* 100%) seen in confocal microscopy studies (Fig. 2, 3), although the difference was statistically significant for all FA or 2OHFA used. As shown in figure 8C and 8D, DRM fractions in control vesicles were composed basically by the Lo forming lipids SM and Cho, although small amounts of the PE and POPC were also found. When vesicles were treated with the 2OHFAs (Fig. 8C) or FAs (Fig. 8 D), the lipid composition of the DRM fractions changed when compared to the control vesicles. Thus, the proportion of the order-inducing lipids Cho and SM increased while the amount of POPC and PE decreased in raft-like microdomains in agreement with previous studies using fluorescence lifetime measurements [14]. Interestingly, neither 2OHFAs nor FAs were found in the DRM fractions (data not shown). Lipid quantification data from vesicles not solubilized with Triton X-100 were used as non-solubilization controls and they clearly showed that virtually all the lipid amount was recovered in the pellet fraction independently of the presence of

DMSO (Fig. 8E). Moreover, the proportion of each lipid from the pellet fraction remained constant in both control samples (Fig. 8F). Altogether the herein presented results suggest that the size of raft-like domains was drastically reduced, so that they could not be seen by confocal microscopy, but they are not eliminated, as about 80% of DRMs are recovered upon FA/2OHFA addition in detergent solubilization studies.

#### 4. Discussion

Membrane Lipid Therapy is a novel therapeutic approach aiming to the regulation of the composition and structure of cell membranes in order to modulate the localization and activity of membrane signaling proteins and subsequently, downstream molecular events [7]. In line with this, the Mediterranean diet is associated with a blood pressure reduction and lower incidence of hypertension, which has been directly associated with OA intake [53]. In addition, omega-3 polyunsaturated fatty acids such as DHA and EPA have been associated with prevention of cardiovascular diseases and cancer [54], while the omega-6 polyunsaturated fatty acid  $\gamma$ LNA is known to possess anti-inflammatory properties [55]. In this scenario, several 2OHFAs have been designed and they have shown a great efficacy for the treatment of cancer (2OHOA), Alzheimer's disease (2OHDHA) and inflammation (2OHARA) [6, 12]. All these effects share common molecular bases, in which the regulation of the membrane lipid structure is a key molecular event that controls protein-lipid and protein-protein interactions at defined domains in order to restore physiological processes in pathological cells.

The aim of the present manuscript was to determine the effect of natural and 2-hydroxylated FA immediately after insertion in the lipid membrane and before becoming part of phospholipid acyl chains [43]. Some previous works have extensively shown the efficacy of OA [56] and 2OHOA [4] in decreasing the lamellar-to-hexagonal transition temperature in lipid membranes. Here, we have demonstrated that the addition of several unsaturated 2OHFAs (besides 2OHOA) or FAs (besides OA) to POPC:PE:SM:Cho (1:1:1:1; mol ratio) membranes, a lipid mixture used as a model to mimic the cell membrane structure, induced re-organization of lipid domains and changes in the lipid composition of membrane regions as compared with control samples. Figures 1-6, show through different experimental approaches, an important re-organization of the membrane structure in the presence of the unsaturated fatty acid derivatives. This fatty acid-induced effect could be due to their tendency to favor negative membrane curvature strain [1, 56]. This ability to modify the membrane biophysical properties explains in part how FAs and 2OHFAs modulate the localization and activity of peripheral and integral membrane proteins and subsequent intracellular cell signaling processes. For instance, polyunsaturated fatty acids have been shown to modulate antigen presentation by changing the organization of lipids and proteins in the plasma membrane [57]. Other drugs, such as the

anesthetic ketamine [20] and the anti-tumor drugs cisplatin and doxorubicin [16, 58], also exert their activities through the modulation of the membrane structure.

Lipid phase separation studies using the NBD-PE self-quenching method (Fig. 1) and FTIR data (Fig. 5-7) showed a destabilization of the membrane structure upon addition of the 2OHFAs derivatives. The decrease of the carbonyl group signal values (1745/1722 ratio) indicated a higher hydration level of samples containing 2OHFAs and FAs molecules (Fig. 5) and the symmetric methylene band signal appeared at higher wavenumber values in presence of 2OHFAs or FAs compared to control samples (Fig. 6), indicating an increase of the hydrocarbon chain mobility. Moreover, the presence of 2OHFAs induced a homogeneous distribution of DiI fluorescence that could be related to a loss of Lo domains as seen in fluorescence confocal microscopy images (Fig. 2) and the size measurements of the Lo and Ld regions (Fig. 3). However, Triton X-100 solubilization assays clearly showed that the amount of Lo structure only decreased from ~50% to ~40% in lipid membranes containing FAs or 2OHFAs (Fig. 8). Although the decrease of the DRM fraction upon incubation with 2OHFAs or FAs (Fig. 8 A, B) was not as marked as suggested by fluorescence and confocal microscopy experiments (Figures 1-3), the reduction of total lipids in Lo microdomains was statistically significant. In addition, the digital analysis of GUV images before and after incubation with 2OHFA derivatives showed no significant differences in the mean fluorescence intensity (Table 1), which prove the fact that the Lo were still present in the lipid bilayer.

Figure 9 shows the proposed model that explains the above mentioned, apparently contradictory results by which the presence of FA and 2OHFA derivatives induces membrane domain reorganization. This model also explains in part the frequent presence of small microdomains in cell membranes, whereas large microdomains like those involved in protein capping (or extensive clustering), are not so frequent. 2OHFAs and FAs most likely caused lipid redistribution and a decrease in the proportion of Lo domains with respect to Ld structures. The fact that no DiI-depleted regions were visualized in GUVs containing 2OHFAs or FAs (Fig. 2-4) in combination with detergent solubilization studies (Fig. 8), suggest that the size of Lo domains drastically decreased below the resolution limit of optical microscopy (*ca.* 200 nm). FTIR data (Fig. 5 and 6) showed a strong destabilization of the lamellar phase of Lo domain ( $T_m$  decrease between 4-12 °C, depending on each fatty acid), which is consistent with the size reduction of Lo domains. On the other hand, the remaining Lo structures became enriched in Cho and, to a lesser extent, in SM as compared to control vesicles which indicates that 2OHFAs and FAs induced changes in Ld-prone (PE, PC) and Lo-prone (SM, Cho) lipid intermixing between membrane domains. These results suggest a rigidifying effect in the lipid raft-like, Lo domains and an increased disorder in Ld regions, which correlates with previous results [37]. There, 2OHFA was observed (i) to increase the *trans*-parinaric acid long lifetime component, indicating that the ordered domains became more ordered and (ii) to decrease the

anisotropy value of 1,6-diphenyl-1,3,5-hexatriene, probing a decrease in the global order of the membrane. This new membrane organization seen in the presence of 2OHOA may modify certain membrane protein activities or protein-protein interactions involved in the propagation of cell signals related to cancer cell differentiation and survival [12].

The cell membrane fluidity increases upon incorporation of unsaturated FAs, whereas it decreases with saturated FAs, which possess rigid hydrocarbon tails [59]. Moreover, the plasma membrane is a cell structure where both permanently and non-permanently associated proteins exert their functions, which at the same time are affected by the surrounding lipid environment [60]. For instance, *c*-Src, a membrane associated tyrosine kinase, is a molecule responsible for the activation of Jun Kinases (JNK) by saturated fatty acids [61]. Saturated fatty acids induce the localization of *c*-Src into membrane sub-domains of reduced fluidity and increased rigidity, where it accumulates in an activated form that eventually leads to ligand-free activation of JNK, a family of proteins implicated in the development of type 2 diabetes, insulin resistance, obesity and atherosclerosis. By contrast, unsaturated fatty acids prevent *c*-Src clustering (in agreement with the above model, Fig. 9), thus inhibiting JNK activation [61]. Saturated FAs also cause PKC-dependent activation of mixed-lineage protein kinases (MLK3) that subsequently causes increased JNK activity by a mechanism that requires the MAP kinase kinases MKK4 and MKK7 [62]. Moreover, PKC $\alpha$  and G-protein interactions with membranes and related signaling events are highly dependent on the membrane structure and microdomain distribution, and 2OHFAs and FAs can influence all these events [5, 8, 13, 16].

Another example of lipid-modulated proteins are heat shock proteins (HSP), which are involved in diverse cell dysfunctions that lead to the development of insulin-resistant diabetes, cancer and the neurodegenerative disease amyotrophic lateral sclerosis. It is known that the physical state of the membrane can modulate the expression of genes encoding for HSPs, thus, leading to different cell responses [63]. For instance, mild changes in temperature could result in a fundamentally altered fluidity of the membrane and, consequently, in the distribution and activity of stress-sensing and stress-signaling proteins within the lipid domains [64].

It has been described a more potent therapeutic effect for the hydroxylated molecules compared to non-hydroxylated FAs [7-9]. For instance, the introduction of a hydroxyl group in the  $\alpha$ -position of oleic acid potentiated the efficacy in the reduction of body weight or blood pressure more than four-fold compared to the non-hydroxylated OA molecule [9, 53]. However, the present data show that both natural and 2-hydroxy fatty acid derivatives exert similar physical changes in lipid membranes, so the hydroxyl group might not be directly responsible for the observed therapeutic effects. An explanation for the increased therapeutic response of these synthetic 2OHFA derivatives is the fact that  $\alpha$ -hydroxy-substituted fatty acids cannot be directly metabolized via the  $\beta$ -oxidation pathway, but must first enter the  $\alpha$ -oxidation pathway where the 2-hydroxy-phytanoyl-CoA lyase is the rate-limiting

enzyme [65]. This enzyme may become rapidly saturated with low substrate concentrations, as it represents a secondary oxidation pathway for non-abundant natural fatty acids and, as a consequence, 2OHFAs may accumulate to a much higher extent than naturally occurring FAs, which are predominantly used as a source of energy [9]. In addition, the extra hydroxyl group may help these FAs establish further hydrogen bonds that may stabilize their presence in the membranes [4]. Other mechanisms involving their incorporation into membrane phospholipids or interaction with membrane proteins should not be discarded. In any case, the results have shown the influence of free FAs and 2OHFA in the lipid membrane structure and organization and also provided relevant information about the differential effect of each lipid species that explain in part the sometimes divergent and often common effect on membrane lipid structure and human health. Thus, saturated FAs/ 2OHFAs have not shown to modulate the membrane biophysical properties or improve human health, whereas their unsaturated analogues have opposite effects on both lipid structure and therapeutic effects.

## **5. Concluding remarks**

The combination of the slow metabolization rate and the capacity to modify lipid organization in membranes, make 2OHFA derivatives potential molecules to revert cell dysfunctions. In this scenario, the modulation of the cell lipid bilayer structure may be part of the mechanism of action of the 2OHFAs. That is, 2-hydroxyoleic acid and related compounds may act as regulators of cell signaling cascades which are initiated in the membrane and that may lead to cell responses such as cell differentiation, cell cycle arrest, apoptosis or autophagy through what has been named as Membrane Lipid Therapy.

## Acknowledgements

The authors thank Dr. Francisco Gavilanes (from Universidad Complutense de Madrid) for the use of the FTIR spectrometer in his laboratory, Dr. Javier Gómez (from Universidad Miguel Hernández) his help developing the “Boltzmann modified equation” and Dr. Manuel Torres for the helpful comments during the preparation of the manuscript. This work was supported by grants from Spanish Ministerio de Ciencia e Innovación grants BIO2010-21132 and Fundación Marathon (PVE) and IPT-010000-2010-16 (XB); PTQ-10-04214 (MI) and PTQ-09-02-02113 (DJL); BFU2008-00602/BMC and CSD2008-00005 (JAE and JMGR).

## Conflict of interest

M.I. and D.J.L. were supported by Torres-Quevedo Research Contracts granted to Lipopharma Therapeutics, S.L. by Ministerio de Economía y Competitividad (Spanish Government). Lipopharma Therapeutics, S.L. is a spin-off, pharmaceutical company from the University of the Balearic Islands.

## Footnotes

<sup>1</sup>Both authors have equally contributed to this work.

<sup>2</sup>Abbreviations:  $\alpha$ LnA,  $\alpha$ -linolenic acid;  $\gamma$ LnA,  $\gamma$ -linolenic acid; ARA, arachidonic acid; Cho, cholesterol; DiI, 1,1'-diiodo-3,3',3''-tetramethylindocarbocyanine perchlorate; DHA, docosahexaenoic acid; DMSO, dimethyl sulfoxide; DRM, detergent resistance membrane; EPA, eicosapentaenoic acid;  $\gamma$ LnA,  $\gamma$ -linolenic acid; GM1, GM1 ganglioside; GUV, giant unilamellar vesicle; HSP, heat shock protein; LA, linoleic acid; Ld, liquid-disordered; Lo, liquid-ordered; LUV, large unilamellar vesicles; MLV, multilamellar vesicles; NBD-PE, 1-oleoyl-2-(12-((7-nitro-2-1,3-benzoxadiazol-4-yl)amino) dodecanoyl)-sn-glycero-3-phosphoethanolamine; OA, oleic acid; PE, phosphatidylethanolamine; POPC, 1-palmitoyl-2-oleoyl-sn-glycero-3-phosphatidylcholine; SA, stearic acid; SM, sphingomyelin; 2OH $\alpha$ LNA, 2-hydroxy- $\alpha$ -linolenic acid; 2OHARA, 2-hydroxyarachidonic acid; 2OHDHA, 2-hydroxy-docosahexaenoic acid; 2OHEPA, 2-hydroxyeicosapentaenoic acid; 2OHFA, 2-hydroxy fatty acid; 2OH $\gamma$ LnA, 2-hydroxy- $\gamma$ -linolenic acid; 2OHLA, 2-hydroxylinoleic acid; 2OHOA, 2-hydroxyoleic acid; 2OHS, 2-hydroxy-stearic acid.

## References

- [1] R.M. Epand, R.F. Epand, N. Ahmed, R. Chen, Promotion of hexagonal phase formation and lipid mixing by fatty acids with varying degrees of unsaturation, *Chem Phys Lipids*, 57 (1991) 75-80.
- [2] V. Demarin, M. Lisak, S. Morovic, Mediterranean diet in healthy lifestyle and prevention of stroke, *Acta Clin Croat*, 50 (2011) 67-77.
- [3] S.J. Baum, P.M. Kris-Etherton, W.C. Willett, A.H. Lichtenstein, L.L. Rudel, K.C. Maki, J. Whelan, C.E. Ramsden, R.C. Block, Fatty acids in cardiovascular health and disease: a comprehensive update, *J Clin Lipidol*, 6 (2012) 216-234.
- [4] F. Barceló, J. Prades, S.S. Funari, J. Frau, R. Alemany, P.V. Escribá, The hypotensive drug 2-hydroxyoleic acid modifies the structural properties of model membranes, *Mol Membr Biol*, 21 (2004) 261-268.
- [5] Q. Yang, R. Alemany, J. Casas, K. Kitajka, S.M. Lanier, P.V. Escribá, Influence of the membrane lipid structure on signal processing via G protein-coupled receptors, *Mol Pharmacol*, 68 (2005) 210-217.
- [6] P.V. Escribá (2006). Use of hydroxyoleic acid and similar compounds in the production of medicaments. Spain. **EP 1435235B1** 05.04.2006. Patent.
- [7] P.V. Escribá, Membrane-lipid therapy: a new approach in molecular medicine, *Trends Mol Med*, 12 (2006) 34-43.
- [8] J. Martínez, A. Gutiérrez, J. Casas, V. Lladó, A. López-Bellán, J. Besalduch, A. Dopazo, P.V. Escribá, The repression of E2F-1 is critical for the activity of Minerval against cancer, *J Pharmacol Exp Ther*, 315 (2005) 466-474.
- [9] O. Vögler, A. López-Bellán, R. Alemany, S. Tofe, M. González, J. Quevedo, V. Pereg, F. Barceló, P.V. Escribá, Structure-effect relation of C18 long-chain fatty acids in the reduction of body weight in rats, *Int J Obes (Lond)*, 32 (2008) 464-473.
- [10] P.V. Escribá (2010). Use of hydroxyoleic acid and related compounds in the manufacture of drugs. USA. **US 7851507B2** Dec 14, 2010. Patent.
- [11] V. Lladó, A. Gutiérrez, J. Martínez, J. Casas, S. Terés, M. Higuera, A. Galmes, C. Saus, J. Besalduch, X. Busquets, P.V. Escribá, Minerval induces apoptosis in Jurkat and other cancer cells, *J Cell Mol Med*, 14 (2010) 659-670.
- [12] S. Terés, V. Lladó, M. Higuera, G. Barceló-Coblijn, M.L. Martín, M.A. Noguera-Salva, A. Marcilla-Etxenike, J.M. García-Verdugo, M. Soriano-Navarro, C. Saus, U. Gómez-Pinedo, X. Busquets, P.V. Escribá, 2-Hydroxyoleate, a nontoxic membrane binding anticancer drug, induces glioma cell differentiation and autophagy, *Proc Natl Acad Sci*, 109 (2012) 8489-8494.



- [13] J. Martínez, O. Vögler, J. Casas, F. Barceló, R. Alemany, J. Prades, T. Nagy, C. Baamonde, P.G. Kasprzyk, S. Terés, C. Saus, P.V. Escribá, Membrane structure modulation, protein kinase C alpha activation, and anticancer activity of minerval, *Mol Pharmacol*, 67 (2005) 531-540.
- [14] G. Barceló-Coblijn, M.L. Martin, R.F. de Almeida, M.A. Noguera-Salva, A. Marcilla-Etxenike, F. Guardiola-Serrano, A. Luth, B. Kleuser, J.E. Halver, P.V. Escribá, Sphingomyelin and sphingomyelin synthase (SMS) in the malignant transformation of glioma cells and in 2-hydroxyoleic acid therapy, *Proc Natl Acad Sci*, 108 (2011) 19569-19574.
- [15] P.V. Escribá, A. Ozaita, C. Ribas, A. Miralles, E. Fodor, T. Farkas, J.A. García-Sevilla, Role of lipid polymorphism in G protein-membrane interactions: nonlamellar-prone phospholipids and peripheral protein binding to membranes, *Proc Natl Acad Sci* 94 (1997) 11375-11380.
- [16] P.V. Escribá, M. Sastre, J.A. García-Sevilla, Disruption of cellular signaling pathways by daunomycin through destabilization of nonlamellar membrane structures, *Proc Natl Acad Sci*, 92 (1995) 7595-7599.
- [17] P.V. Escribá, P. Morales, A. Smith, Membrane phospholipid reorganization differentially regulates metallothionein and heme oxygenase by heme-hemopexin, *DNA Cell Biol*, 21 (2002) 355-364.
- [18] D.J. López, M. Egado-Gabas, I. López-Montero, J.V. Busto, J. Casas, M. Garnier, F. Monroy, B. Larijani, F.M. Goñi, A. Alonso, Accumulated Bending Energy Elicits Neutral Sphingomyelinase Activity in Human Red Blood Cells, *Biophys J*, 102 (2012) 2077-2085.
- [19] G. Lenaz, Lipid fluidity and membrane protein dynamics, *Biosci Rep*, 7 (1987) 823-837.
- [20] H. Jerabek, G. Pabst, M. Rappolt, T. Stockner, Membrane-mediated effect on ion channels induced by the anesthetic drug ketamine, *J Am Chem Soc*, 132 (2010) 7990-7997.
- [21] A. Kopp Lugli, C.S. Yost, C.H. Kindler, Anaesthetic mechanisms: update on the challenge of unravelling the mystery of anaesthesia, *Eur J Anaesthesiol*, 26 (2009) 807-820.
- [22] J.P. Huidobro-Toro, R.A. Harris, Brain lipids that induce sleep are novel modulators of 5-hydroxytryptamine receptors, *Proc Natl Acad Sci*, 93 (1996) 8078-8082.
- [23] B. Stancevic, R. Kolesnick, Ceramide-rich platforms in transmembrane signaling, *FEBS letters*, 584 (2010) 1728-1740.
- [24] M.B. Ruíz-Argüello, M.P. Veiga, J.L. Arrondo, F.M. Goñi, A. Alonso, Sphingomyelinase cleavage of sphingomyelin in pure and mixed lipid membranes. Influence of the physical state of the sphingolipid, *Chem Phys Lipids*, 114 (2002) 11-20.
- [25] K. Simons, E. Ikonen, Functional rafts in cell membranes, *Nature*, 387 (1997) 569-572.
- [26] V. Michel, M. Bakovic, Lipid rafts in health and disease, *Biology of the cell / under the auspices of the European Cell Biology Organization*, 99 (2007) 129-140.

- [27] R. Ehehalt, P. Keller, C. Haass, C. Thiele, K. Simons, Amyloidogenic processing of the Alzheimer beta-amyloid precursor protein depends on lipid rafts, *J Cell Biol*, 160 (2003) 113-123.
- [28] M. Hashimoto, T. Takenouchi, E. Rockenstein, E. Masliah, Alpha-synuclein up-regulates expression of caveolin-1 and down-regulates extracellular signal-regulated kinase activity in B103 neuroblastoma cells: role in the pathogenesis of Parkinson's disease, *J Neurochem*, 85 (2003) 1468-1479.
- [29] A. Taraboulos, M. Scott, A. Semenov, D. Avrahami, L. Laszlo, S.B. Prusiner, Cholesterol depletion and modification of COOH-terminal targeting sequence of the prion protein inhibit formation of the scrapie isoform, *J Cell Biol*, 129 (1995) 121-132.
- [30] E.C. Jury, P.S. Kabouridis, F. Flores-Borja, R.A. Mageed, D.A. Isenberg, Altered lipid raft-associated signaling and ganglioside expression in T lymphocytes from patients with systemic lupus erythematosus, *J Clin Invest*, 113 (2004) 1176-1187.
- [31] G. Del Real, S. Jiménez-Baranda, R.A. Lacalle, E. Mira, P. Lucas, C. Gómez-Mouton, A.C. Carrera, A.C. Martínez, S. Manes, Blocking of HIV-1 infection by targeting CD4 to nonraft membrane domains, *J Exp Med*, 196 (2002) 293-301.
- [32] S.K. Patra, Dissecting lipid raft facilitated cell signaling pathways in cancer, *Biochim Biophys Acta*, 1785 (2008) 182-206.
- [33] T. Murai, The role of lipid rafts in cancer cell adhesion and migration, *International journal of cell biology*, 2012 (2012) 763283.
- [34] L.D. Mayer, M.J. Hope, P.R. Cullis, Vesicles of variable sizes produced by a rapid extrusion procedure, *Biochim Biophys Acta*, 858 (1986) 161-168.
- [35] M.B. Ruíz-Argüello, G. Basañez, F.M. Goñi, A. Alonso, Different effects of enzyme-generated ceramides and diacylglycerols in phospholipid membrane fusion and leakage, *J Biol Chem*, 271 (1996) 26616-26621.
- [36] D. Hoekstra, Role of lipid phase separations and membrane hydration in phospholipid vesicle fusion, *Biochem*, 21 (1982) 2833-2840.
- [37] A. Marcilla-Etxenike, M.L. Martin, M.A. Noguera-Salva, J.M. Garcia-Verdugo, M. Soriano-Navarro, I. Dey, P.V. Escriba, X. Busquets, 2-Hydroxyoleic acid induces ER stress and autophagy in various human glioma cell lines, *PLoS one*, 7 (2012) e48235.
- [38] I.M. Angelova, D.S. Dimitrov, Liposome electroformation, *Faraday Discuss Chem Soc* 81, 303-311., (1986).
- [39] M. Ibarguren, D.J. López, L.R. Montes, J. Sot, A.I. Vasil, M.L. Vasil, F.M. Goñi, A. Alonso, Imaging the early stages of phospholipase C/sphingomyelinase activity on vesicles containing coexisting ordered-disordered and gel-fluid domains, *J Lipid Res*, 52 (2011) 635-645.

- [40] F. Barceló, J. Prades, J.A. Encinar, S.S. Funari, O. Vögler, J.M. González-Ros, P.V. Escribá, Interaction of the C-terminal region of the Ggamma protein with model membranes, *Biophys J*, 93 (2007) 2530-2541.
- [41] N. Kahya, D. Scherfeld, K. Bacia, B. Poolman, P. Schwille, Probing lipid mobility of raft-exhibiting model membranes by fluorescence correlation spectroscopy, *J Biol Chem*, 278 (2003) 28109-28115.
- [42] P. Akuthota, R.C. Melo, L.A. Spencer, P.F. Weller, MHC Class II and CD9 in Human Eosinophils Localize to Detergent-Resistant Membrane Microdomains, *Am J Respir Cell Mol Biol*, 46 (2012) 188-195.
- [43] S.R. Shaikh, A.C. Dumaul, A. Castillo, D. LoCascio, R.A. Siddiqui, W. Stillwell, S.R. Wassall, Oleic and docosahexaenoic acid differentially phase separate from lipid raft molecules: a comparative NMR, DSC, AFM, and detergent extraction study, *Biophys J*, 87 (2004) 1752-1766.
- [44] J. Sot, M. Ibarguren, J.V. Busto, L.R. Montes, F.M. Goñi, A. Alonso, Cholesterol displacement by ceramide in sphingomyelin-containing liquid-ordered domains, and generation of gel regions in giant lipidic vesicles, *FEBS letters*, 582 (2008) 3230-3236.
- [45] R.F. de Almeida, L.M. Loura, A. Fedorov, M. Prieto, Lipid rafts have different sizes depending on membrane composition: a time-resolved fluorescence resonance energy transfer study, *J Mol Biol*, 346 (2005) 1109-1120.
- [46] D. Huster, P. Muller, K. Arnold, A. Herrmann, Dynamics of membrane penetration of the fluorescent 7-nitrobenz-2-oxa-1,3-diazol-4-yl (NBD) group attached to an acyl chain of phosphatidylcholine, *Biophys J*, 80 (2001) 822-831.
- [47] H.H. Mantsch, R.N. McElhaney, Phospholipid phase transitions in model and biological membranes as studied by infrared spectroscopy, *Chem Phys Lipids*, 57 (1991) 213-226.
- [48] H.H. Mantsch, A. Martin, D.G. Cameron, Characterization by infrared spectroscopy of the bilayer to nonbilayer phase transition of phosphatidylethanolamines, *Biochem*, 20 (1981) 3138-3145.
- [49] P.L. Yeagle, W.C. Hutton, R.B. Martin, Sphingomyelin multiple phase behavior as revealed by multinuclear magnetic resonance spectroscopy, *Biochem*, 17 (1978) 5745-5750.
- [50] R.M. Epand, R.F. Epand, Non-raft forming sphingomyelin-cholesterol mixtures, *Chem Phys Lipids*, 132 (2004) 37-46.
- [51] M.P. Veiga, J.L. Arrondo, F.M. Goñi, A. Alonso, D. Marsh, Interaction of cholesterol with sphingomyelin in mixed membranes containing phosphatidylcholine, studied by spin-label ESR and IR spectroscopies. A possible stabilization of gel-phase sphingolipid domains by cholesterol, *Biochem*, 40 (2001) 2614-2622.

- [52] R.N.A.H. Lewis, McElhaney, Fourier transform infrared spectroscopy in the study of hydrated lipids and lipid bilayer membranes., in: H.H. Mantsch, D. Chapman (Eds.) *Infrared Spectroscopy of Biomolecules.*, Wiley-Liss, New York, 1996, pp. 159 - 202.
- [53] S. Terés, G. Barceló-Coblijn, M. Benet, R. Álvarez, R. Bressani, J.E. Halver, P.V. Escribá, Oleic acid content is responsible for the reduction in blood pressure induced by olive oil, *Proc Natl Acad Sci*, 105 (2008) 13811-13816.
- [54] C.J. Lavie, R.V. Milani, M.R. Mehra, H.O. Ventura, Omega-3 polyunsaturated fatty acids and cardiovascular diseases, *J Am Coll Cardiol*, 54 (2009) 585-594.
- [55] R. Kapoor, Y.S. Huang, Gamma linolenic acid: an antiinflammatory omega-6 fatty acid, *Curr Pharm Biotechnol*, 7 (2006) 531-534.
- [56] J. Prades, S.S. Funari, P.V. Escribá, F. Barceló, Effects of unsaturated fatty acids and triacylglycerols on phosphatidylethanolamine membrane structure, *J Lipid Res*, 44 (2003) 1720-1727.
- [57] S.R. Shaikh, M. Edidin, Polyunsaturated fatty acids and membrane organization: elucidating mechanisms to balance immunotherapy and susceptibility to infection, *Chem Phys Lipids Chem Phys Lipids*, 153 (2008) 24-33.
- [58] A. Rebillard, X. Tekpli, O. Meurette, O. Sergeant, G. LeMoigne-Muller, L. Vernhet, M. Gorria, M. Chevanne, M. Christmann, B. Kaina, L. Counillon, E. Gulbins, D. Lagadic-Gossmann, M.T. Dimanche-Boitrel, Cisplatin-induced apoptosis involves membrane fluidification via inhibition of NHE1 in human colon cancer cells, *Cancer Res*, 67 (2007) 7865-7874.
- [59] S. Yehuda, S. Rabinovitz, R.L. Carasso, D.I. Mostofsky, The role of polyunsaturated fatty acids in restoring the aging neuronal membrane, *Neurobiol Aging*, 23 (2002) 843-853.
- [60] F.M. Goñi, Non-permanent proteins in membranes: when proteins come as visitors (Review), *Mol Membr Biol*, 19 (2002) 237-245.
- [61] R.G. Holzer, E.J. Park, N. Li, H. Tran, M. Chen, C. Choi, G. Solinas, M. Karin, Saturated fatty acids induce c-Src clustering within membrane subdomains, leading to JNK activation, *Cell*, 147 (2011) 173-184.
- [62] A. Jaeschke, R.J. Davis, Metabolic stress signaling mediated by mixed-lineage kinases, *Mol Cell*, 27 (2007) 498-508.
- [63] L. Vigh, B. Maresca, J.L. Harwood, Does the membrane's physical state control the expression of heat shock and other genes?, *Trends Biochem Sci*, 23 (1998) 369-374.
- [64] L. Vigh, I. Horvath, B. Maresca, J.L. Harwood, Can the stress protein response be controlled by 'membrane-lipid therapy'?, *Trends Biochem Sci*, 32 (2007) 357-363.
- [65] V. Foulon, M. Sniekers, E. Huysmans, S. Asselberghs, V. Mahieu, G.P. Mannaerts, P.P. Van Veldhoven, M. Casteels, Breakdown of 2-hydroxylated straight chain fatty acids via peroxisomal 2-

hydroxyphytanoyl-CoA lyase: a revised pathway for the alpha-oxidation of straight chain fatty acids, J Biol Chem, 280 (2005) 9802-9812.

ACCEPTED MANUSCRIPT

## Figure legends

**Fig. 1.** Effects of 2OHFAs on NBD-PE fluorescence intensity in LUVs. (A) Large Unilamellar Vesicles composed of POPC:SM:PE:Cho (1:1:1:1 mol ratio) + 5 % NBD-PE were incubated with 15, 30 and 45 mol% of 2OHOA in DMSO. Bar diagrams show the fluorescence intensity changes after addition of 15 mol% of (B) 2-hydroxylated and (C) non-hydroxylated fatty acid molecules. Bars show mean fluorescence values of 3 measurements  $\pm$  SD. \*  $p < 0.05$ , \*\*  $< 0.01$  and \*\*\*  $< 0.001$ . # means  $p < 0.05$  or greater significance compared to the control experiment (DMSO). § means  $p < 0.05$  or greater significance compared to (B) OA or LA and (C) 2OHOA.  $\lambda_{ex} = 475$  nm and  $\lambda_{em} = 530$  nm.

**Fig. 2.** Effects of 2OHFAs on membrane domain organization by confocal microscopy. GUVs composed of POPC:SM:PE:Cho (1:1:1:1; mol ratio) were incubated with 0.135 mM 2OHSA, 2OHOA, 2OHARA and 2OHDHA. Ld domains were stained with DiI (yellow) while Lo structures appear as dark domains. Representative images were taken at different times after addition of the fatty acid. DMSO was used as a negative control. Bar = 10  $\mu$ m.

**Fig. 3.** Quantification of lipid domains in GUV after incubation with 2OHFAs. Percentage of Lo and Ld lipid domains was quantitated from confocal fluorescence images of GUVs at different times after addition of 2OHSA, 2OHOA, 2OHARA and 2OHDHA. Data show average values of Lo and Ld domains from 8-10 vesicles  $\pm$  S. D.

**Fig. 4.** Effects of FAs on membrane domain organization by confocal microscopy. GUVs composed of POPC:SM:PE:Cho (1:1:1:1; mol ratio) were incubated with SA, OA, ARA and DHA. Ld domains are stained with DiI (yellow) while Lo phases appear as dark domains. Representative images were taken before and after 180 seconds of addition of FAs. DMSO was used as a negative control. Bar = 10  $\mu$ m.

**Fig. 5.** FTIR temperature profiles of POPC:SM:PE:Cho (1:1:1:1; mol ratio) in the presence or absence of 15 mol% FA or 2OHFA. Temperature-dependent changes (A-C) in the intensity band ratio of the carbonyl stretching modes and in (D-F) the maximum frequency of the CH<sub>2</sub> symmetric stretching. FTIR spectra are shown for (A, D) 2OHOA and OA, (B, E) 2OHARA and ARA and (C, F) 2OHDHA and DHA added to matrices of POPC:PE:SM:Cho bilayers. Quaternary POPC:PE:SM:Cho (control, ■) mixture in the presence of 15 mol% FA (●) or 15 mol% 2OHFA (Δ) are shown in each panel. Melting temperatures for each curve are indicated with arrows. The solid line represents the best fits of experimental data to a modified sigmoid equation (see Materials and Methods).

**Fig. 6.** Temperature dependence of “sphingomyelin amide I” infrared band. The frequency of the maximum “sphingomyelin amide I” band is plotted versus temperature for matrices of POPC:PE:SM:Cho lipid bilayers alone (■) and with FA(●) and 2OHFA (Δ): (A) 2OHOA and OA, (B) 2OHARA and ARA and (C) 2OHDHA and DHA. Melting temperatures for each curve are indicated with arrows in all panels. The solid line represents the best fits of experimental data to a modified sigmoid equation (see Materials and Methods).

**Fig. 7.** Lipids infrared spectra. (A) Infrared spectra for POPC:PE:SM:Cho (1:1:1:1; mol ratio) in the absence (black line) or presence of 15 mol% OA (blue line) or 15 mol% 2 OHOA (red line), in the carbonyl (1770-1680  $\text{cm}^{-1}$ ) region at 23 °C. (B) Temperature-dependent behavior of the methylene symmetric stretching (2865-2830  $\text{cm}^{-1}$ ) and methyl antisymmetric (2947-2878  $\text{cm}^{-1}$ ) infrared spectrum of POPC:PE:SM:Cho (1:1:1:1; mol ratio) with 2OHOA; there are 27 individual spectra, each about 2 °C apart. (C) Infrared spectra of carbonyl and “sphingomyelin amide I” bands for POPC:PE:SM:Cho (1:1:1:1; mol ratio) with 2OHOA at 23 °C (dashed line) and 73 °C (continuous line). Each spectrum of panel C showed the maximum frequency of the “sphingomyelin amide I” band. In all cases samples were suspended in 10 mM Hepes, pH 7.4, containing 1 mM EDTA, 100 mM NaCl.  $\text{CaF}_2$  windows were used in the spectrometer cell.

**Fig. 8.** Effect of 2OHFAs on DRM (i.e., Lo domains) proportion in model membranes. Vesicles composed of POPC:SM:PE:Cho (1:1:1:1; mol ratio) containing 1 mol% GM1 were incubated in the presence or absence of 15 mol% 2OHOA, 2OHARA and 2OHDHA and solubilized with TX100 at 4 °C for 60 min. (A, B) The lipid composition from the detergent resistant fractions (DRM) was quantified by thin layer chromatography and compared with control vesicles in the presence of 2OHFAs and non-hydroxylated FAs. (C, D) The different lipid species contained in the DRM fraction were quantified and compared to control vesicles (solid bars) after treatment with 2OHOA (gray bars), 2OHARA (open bars) and 2OHDHA (striped bars) in panel C and with OA (gray bars), ARA (open bars) and DHA (striped bars) in panel D. (E) Vesicles treated in absence of Triton X-100 and DMSO (C-/-) or in absence of Triton X-100 but in presence of DMSO (C-/+). The vesicles were processed as indicated in Experimental Procedures and the amount of total lipids in the pellet fraction after centrifugation was quantified densitometrically. (F) Densitometric quantification of each lipid species in the pellet fraction of C-/- (gray bars) and C-/+ (white bars) vesicles. Bars represent means of at least 3 independent experiments  $\pm$  SEM. \* means  $p < 0.05$ , \*\*  $< 0.01$  and \*\*\*  $< 0.001$ , compared to control vesicles.

**Fig. 9.** Model for the lipid domain reorganization induced by 2OHFAs on membranes. Lo/Ld domain ratio is reduced from *ca.* 50 to *ca.* 40% of the total membrane surface upon insertion of 15 mol% 2OHFA derivatives in a lipid membrane. The size of Lo domain decreases so that they may not be observed under a fluorescence confocal microscope; however, the presence of Lo domains is supported by the measure of a relevant DRM fraction after detergent solubilization .

ACCEPTED MANUSCRIPT



Table 1. Change of overall fluorescence intensity in GUVs upon incubation with 2OHFA.

	${}^aF_{0s}$	$F_{180s}$
2OHOA	$16.0 \pm 3.3$	$16.5 \pm 3.7$
2OHARA	$21.6 \pm 2.6$	$21.8 \pm 3.3$
2OHDHA	$10.2 \pm 0.9$	$12.5 \pm 1.3$

<sup>a</sup>F means mean fluorescence intensity (arbitrary units) at time 0 s and 180 s after addition of 2OHFA derivatives.

ACCEPTED MANUSCRIPT

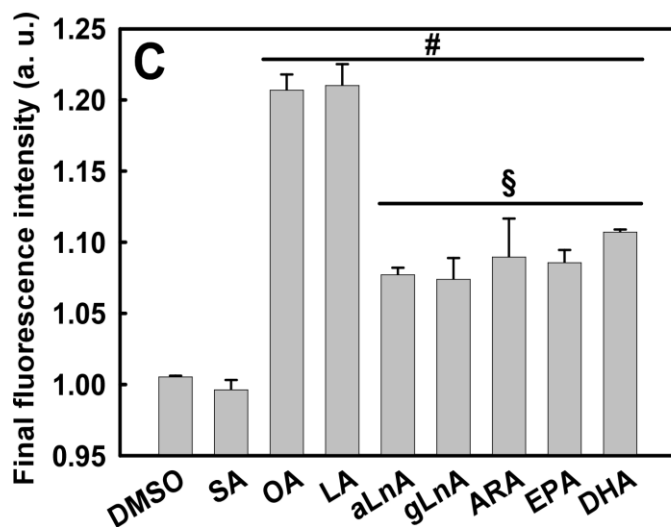
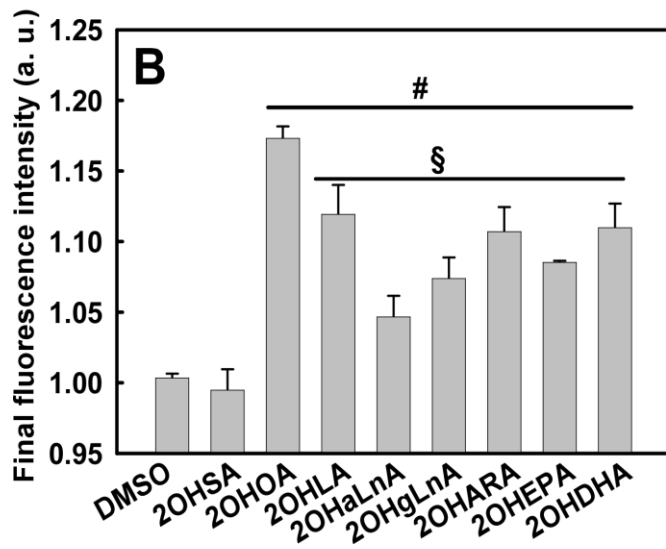
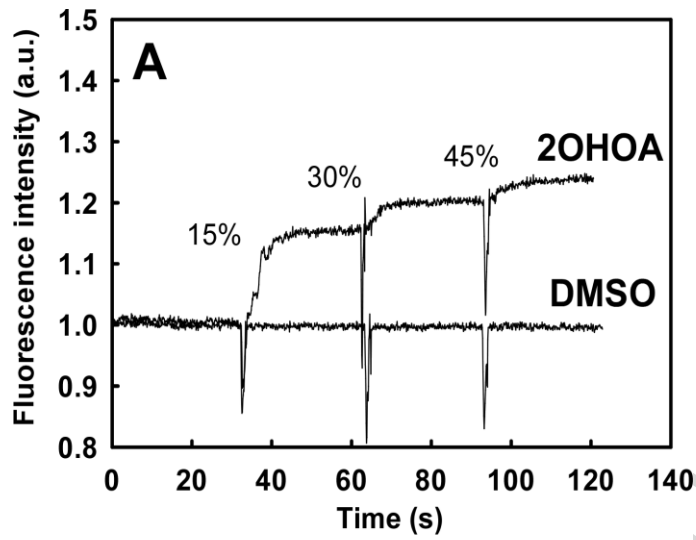


Figure 1

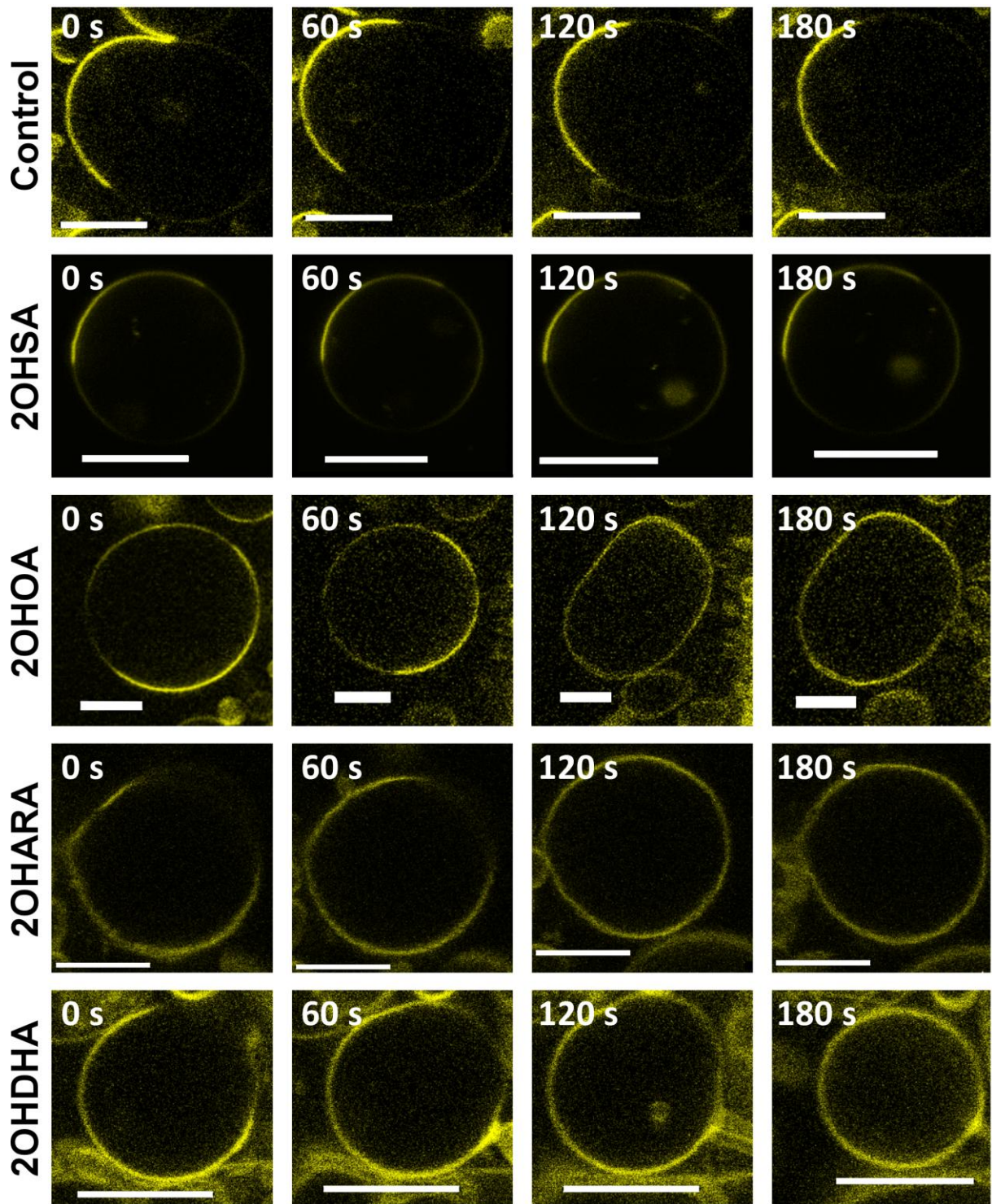


Figure 2

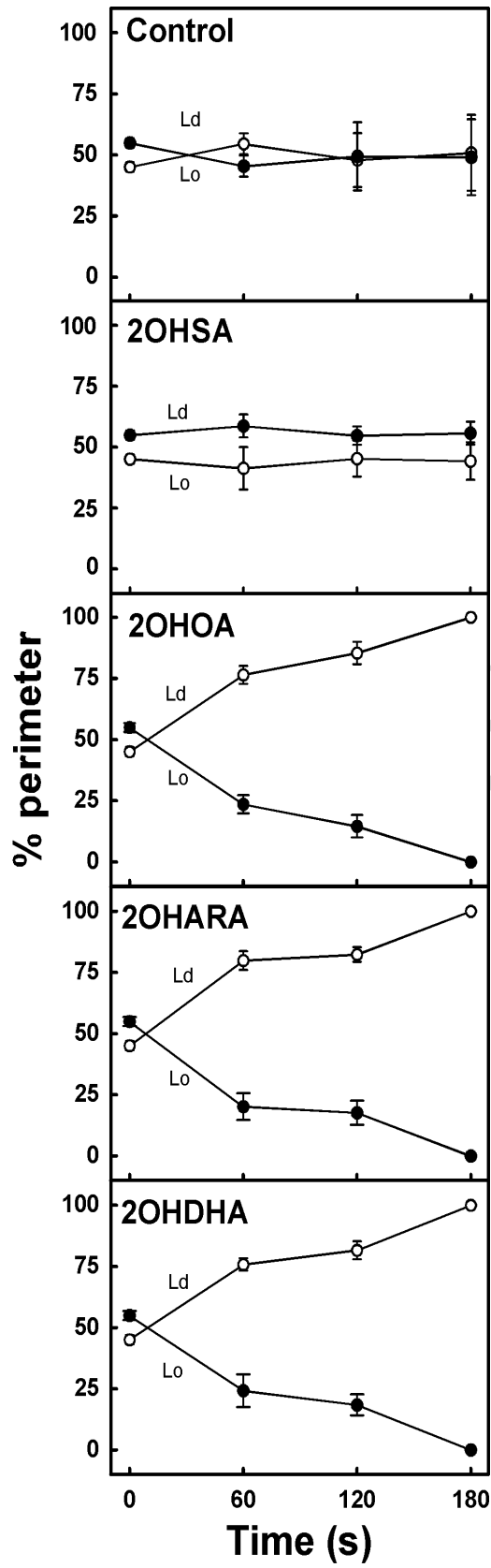
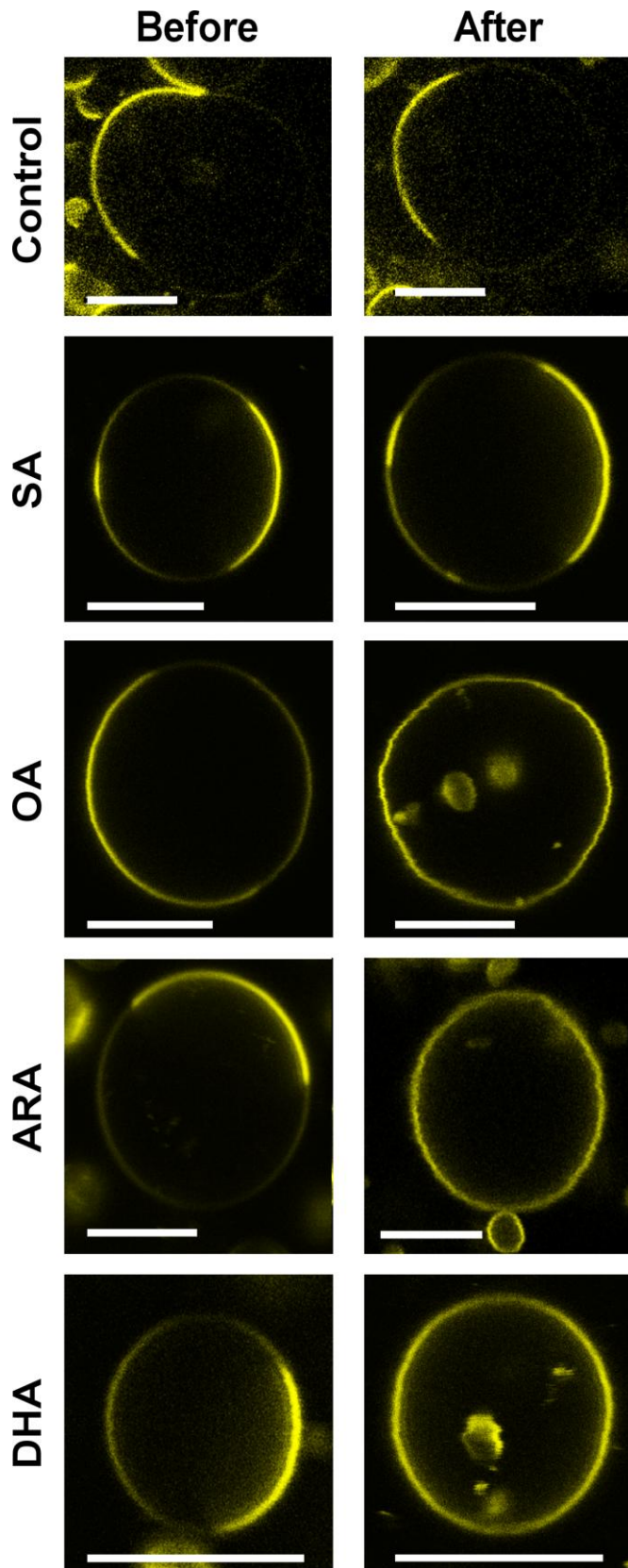


Figure 3



SCRIPT

Figure 4

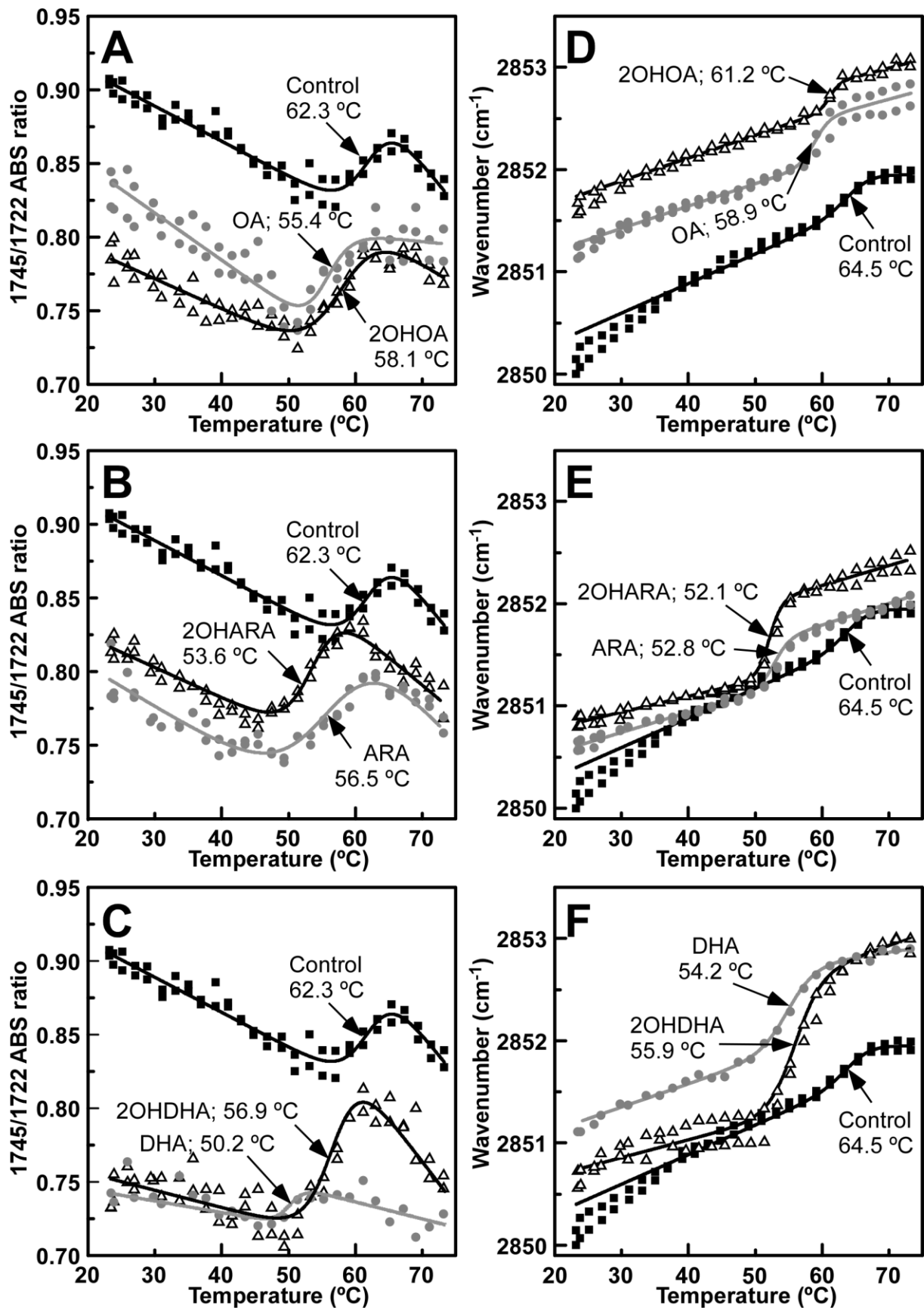


Figure 5

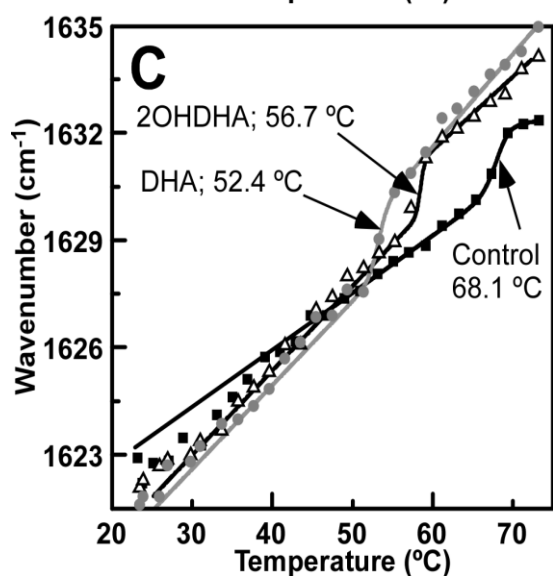
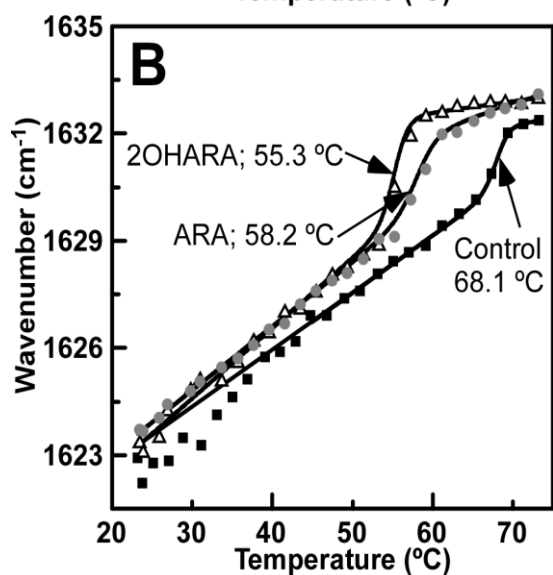
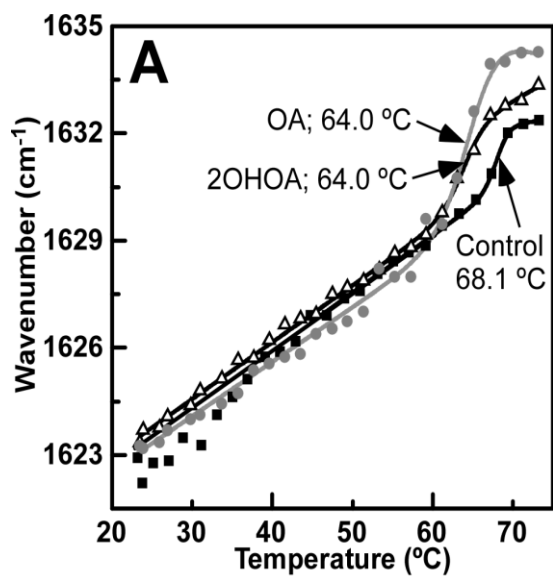


Figure 6



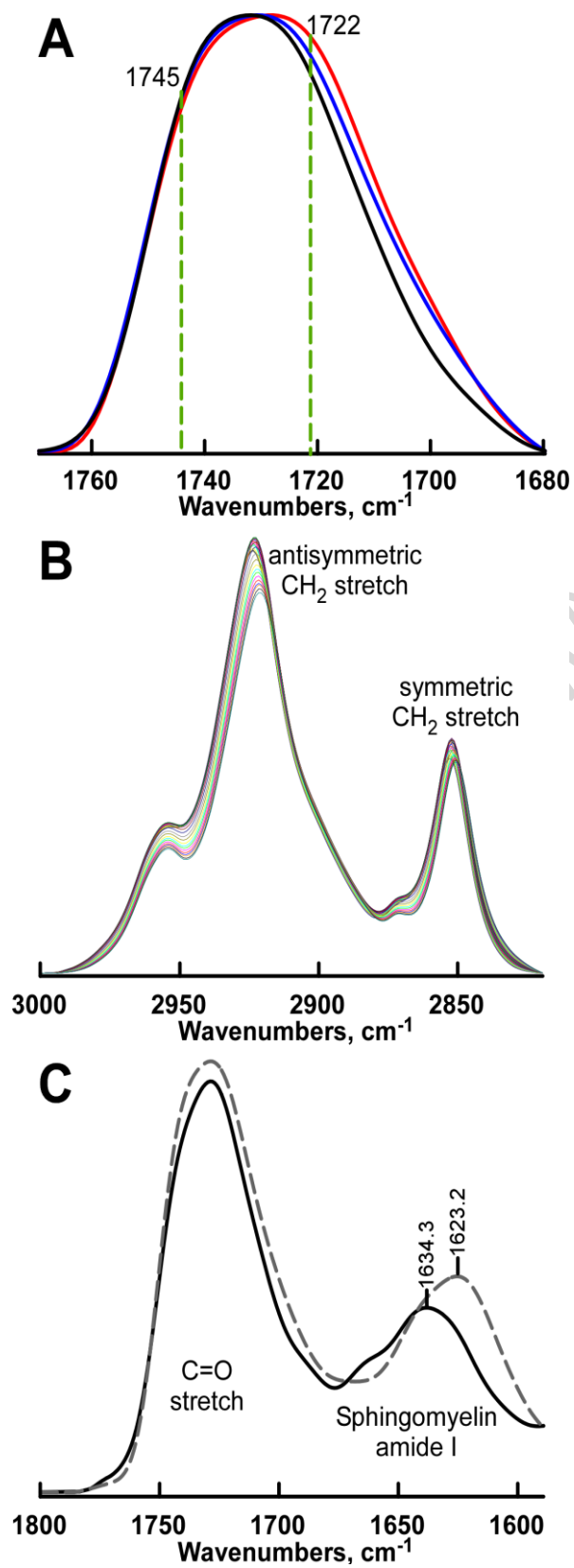


Figure 7



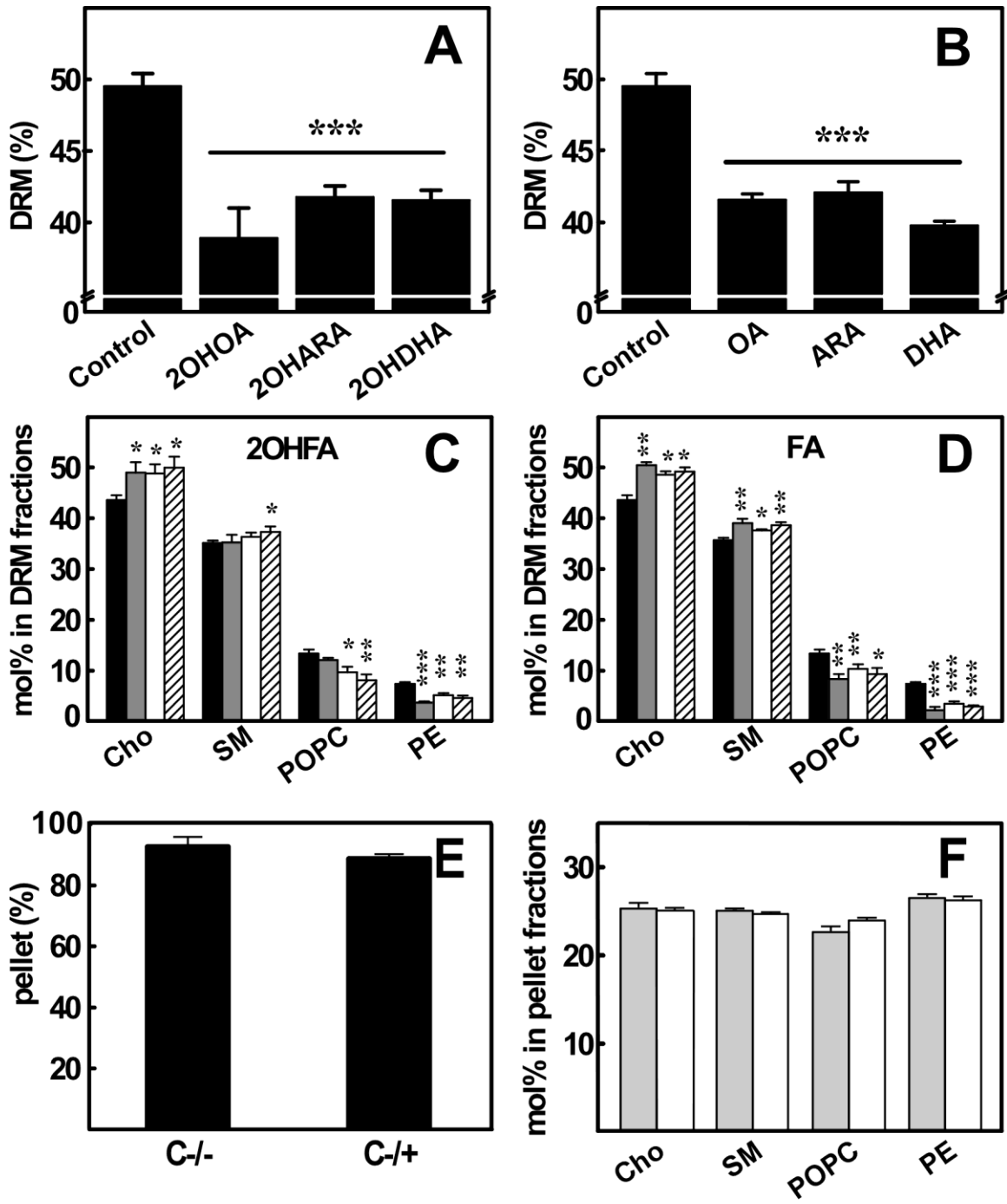


Figure 8

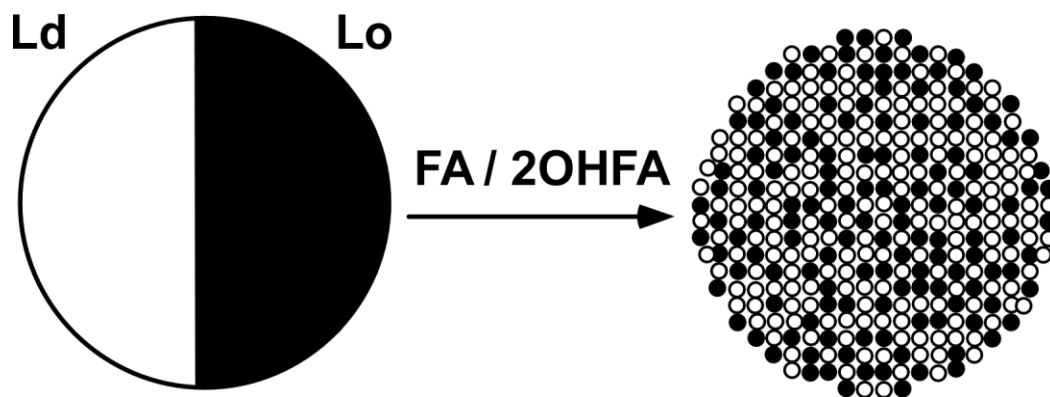
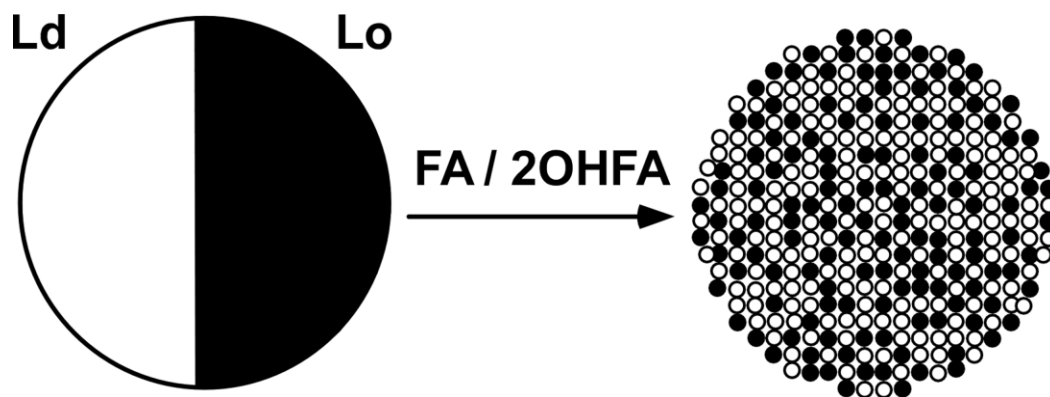


Figure 9

ACCEPTED MANUSCRIPT



Graphical Abstract

ACCEPTED MANUSCRIPT

## Highlights

- 2OHFAs have shown therapeutic effects against cancer, hypertension or Alzheimer's disease.
- 2OHFAs modulate the membrane lipid structure and the proportion of Lo/Ld microdomains.
- Both natural and 2-hydroxylated FAs exert similar structural effects in lipid membranes.
- The low rate of metabolism of 2OHFAs may favor their therapeutic effect compared with natural FAs.
- These results explain in part the mechanism of action of 2OHFAs against various diseases.

ACCEPTED MANUSCRIPT